British Journal of Mathematics & Computer Science
18(5): 1-26, 2016, Article no.BJMCS.27221
ISSN: 2231-0851

SCIENCEDOMAIN *international*
www.sciencedomain.org

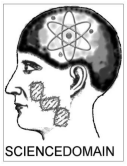

Effects of Hall Current and Rotation on Unsteady MHD Natural Convection Flow Past a Vertical Flat Plate with Ramped Wall Temperature and Heat Absorption

K. K. Pandit[1*], D. Sarma[1] and A. K. Deka[2]

[1] Department of Mathematics, Cotton College, Guwahati 781001, Assam, India.
[2]Department of Mathematics, Gauhati University, Guwahati, 781014, Assam, India.

Authors' contributions

This work was carried out in collaboration between all authors. Author KKP conceptualize the idea of research, formulation of the problem and computed the results. Author DS edited the paper and confirmed the well-posed-ness of the problem, directed the general setup of the paper and author AKD proof read the manuscript. All authors read and approved the final manuscript.

Article Information

DOI: 10.9734/BJMCS/2016/27221
Editor(s):
(1) Sun-Yuan Hsieh, Department of Computer Science and Information Engineering, National Cheng Kung University, Taiwan.
(2) Jacek Dziok, Institute of Mathematics, University of Rzeszow, Poland.
(3) Tian-Xiao He, Department of Mathematics and Computer Science, Illinois Wesleyan University, USA.
Reviewers:
(1) S. M. Arifuzzaman, Khulna University, Bangladesh .
(2) Mainul Hoque, University of Newcastle, Australia.
(3) Houari Ameur, University Center Ahmed Salhi, Ctr Univ Naâma, Algeria.
(4) Anonymous, University of the Witwatersrand, Johannesburg, South Africa.
Complete Peer review History: http://www.sciencedomain.org/review-history/16081

Original Research Article

Received: 24th May 2016
Accepted: 2nd August 2016
Published: 7th September 2016

Abstract

In the present study, the effects of Hall current and rotation on an unsteady Magneto-Hydrodynamic (MHD) free convection heat and mass transfer of an electrically conducting, viscous, incompressible and heat absorbing fluid flow past a vertical infinite flat plate embedded in non-Darcy porous medium is investigated. The flow is induced by a general time-dependent movement of the vertical plate, and the cases of ramped temperature and isothermal plates are studied. Exact solution of the governing time-dependent boundary layer equations for the momentum, energy and concentration were obtained in closed form by using Laplace Transform technique. Expressions for skin friction due to primary and secondary flows and Nusselt number are derived for both ramped temperature and isothermal plates. Expression for Sherwood number is also derived. Some applications of practical interest for different types of plate

**Corresponding author: E-mail: kamalesh.pandit@yahoo.co.in;*

motions viz. plate moving with uniform velocity, plate moving with uniform acceleration and plate moving with periodic acceleration are discussed. The numerical values of fluid velocity, fluid temperature and species concentration are displayed graphically whereas the numerical values of skin friction, the Nusselt number and the Sherwood number are presented in tabular form for various values of pertinent flow parameters for both ramped temperature and isothermal plates. It is found that the primary fluid velocity decreases with increasing values of Hall current parameter whereas it has reverse effect on secondary fluid velocity, in all types of motion of plate discussed. The Primary fluid velocity decreases with the increasing value of rotation parameter whereas it has reverse effect on secondary fluid velocity. Hall current tends to reduce the primary skin friction for both ramped temperature and isothermal plate whereas it has reverse effect on secondary skin friction.

Keywords: Free convection; MHD; hall current; chemical reaction; thermal radiation; porous medium.

Nomenclatures

Symbols		*Meaning*	*Symbols*		*Meaning*
B_0	:	*The strength of uniform transverse magnetic field*	q_r	:	*Radiative heat flux*
C	:	*Species concentration*	Q_0	:	*The heat absorption coefficient*
Cp	:	*Specific heat at constant pressure*	T	:	*The temperature of the fluid (Kelvin; K)*
D	:	*Chemical molecular mass diffusivity*	t_o	:	*The characteristics time*
g	:	*Acceleration due to gravity*	(u,v)	:	*Velocity components*
Gm	:	*The solutal Grashof number*	(x,y)	:	*Transverse and normal directions*
Gr	:	*The thermal Grashof number*	β	:	*The volumetric coefficient of thermal expansion*
k	:	*Thermal conductivity*	β'	:	*The volumetric coefficient of expansion for concentration*
K_1	:	*Permeability of the porous medium*	σ	:	*The electrical conductivity*
Kr	:	*Chemical reaction parameter*	ω_e	:	*Cyclotron frequency*
k_1	:	*Rosseland mean absorption co-efficient*	τ_e	:	*Electron collision time*
M	:	*The magnetic parameter*	σ_1	:	*Stefan-Boltzmann constant*
N	:	*The radiation parameter*	ρ	:	*The fluid density*
Pr	:	*The Prandtl number*	υ	:	*The kinematic viscosity*
$\mathrm{m} = \omega_e \tau_e$	:	*Hall current parameter*			

1 Introduction

The study of natural convection flow induced by the simultaneous action of thermal and solutal buoyancy forces acting over bodies with different geometries in a fluid with porous medium is common in many natural phenomena and has wide range of industrial applications. For example, the presence of pure air or water is impossible because some foreign mass may be present either naturally or mixed with air or water due to industrial emissions, in atmospheric flows. Natural processes such as attenuation of toxic waste in water bodies, vaporization of mist and fog, photosynthesis, transpiration, sea-wind formation, drying of porous solids, and formation of ocean currents [1] occur due to thermal and solutal buoyancy forces developed as a result of difference in temperature or concentration or a combination of these two. Such configuration is also encountered in several practical systems for industry based applications viz. cooling of

molten metals, heat exchanger devices, petroleum reservoirs, insulation systems, filtration, nuclear waste repositories, chemical catalytic reactors and processes, desert coolers, frost formation in vertical channels, wet bulb thermometers, etc. Considering the importance of such fluid flow problems, extensive and in-depth research works have been carried out by several researchers [2–5] in the past.

The study of hydromagnetic natural convection flow with heat and mass transfer in porous and non-porous media has drawn considerable attentions of several researchers due to its applications in geophysics, astrophysics, aeronautics, meteorology, electronics, chemical, and metallurgy and petroleum industries. Magneto-Hydrodynamic (MHD) natural convection flow of an electrically conducting fluid in a fluid with porous medium has also been successfully exploited in crystal formation. Oreper and Szekely [6] have found that the presence of a magnetic field can suppress natural convection currents and the strength of magnetic field is one of the important factors in reducing non-uniform composition thereby enhancing quality of the crystal. In addition to it, the thermal physics of hydromagnetic problems with mass transfer is of much significance in MHD flow-meters, MHD energy generators, MHD pumps, controlled thermo-nuclear reactors, MHD accelerators, etc. Keeping in view the importance of such study, Hossain and Mandal [7] investigated mass transfer effects on unsteady hydromagnetic free convection flow past an accelerated vertical porous plate. Jha [8] studied hydromagnetic free convection and mass transfer flow past a uniformly accelerated vertical plate through a porous medium when magnetic field is fixed with the moving plate. Chen [9] analyzed combined heat and mass transfer in MHD free convection flow from a vertical surface with Ohmic heating and viscous dissipation. Chamkha [10] investigated unsteady MHD convection flow with heat and mass transfer past a semi-infinite vertical permeable moving plate in a uniform porous medium with heat absorption. Eldabe et al. [11] discussed unsteady MHD flow of a viscous and incompressible fluid with heat and mass transfer in a porous medium near a moving vertical plate with time-dependent velocity. Investigation of hydromagnetic natural convection flow in a rotating medium is of considerable importance due to its application in various areas of astrophysics, geophysics and fluid engineering viz. maintenance and secular variations in Earth's magnetic field due to motion of Earth's liquid core, structure of the magnetic stars, internal rotation rate of the Sun, turbo machines, solar and planetary dynamo problems, rotating drum separators for liquid metal MHD applications, rotating MHD generators, etc. Taking into consideration the importance of such study, unsteady hydromagnetic natural convection flow past a moving plate in a rotating medium is studied by a number of researchers such as the studies of Singh [12,13], Raptis and Singh [14] and Singh et al. [15].

The effect of thermal radiation and chemical reaction on MHD boundary layer flow has become important in several industrial, scientific and engineering fields. The growing need for chemical reaction in chemical and hydrometallurgical industries requires the study of heat and mass transfer with chemical reaction. There are many transport processes that are governed by the combined action of buoyancy forces due to both thermal and mass diffusion in presence of the chemical reaction. These processes are observed in nuclear reactor safety and combustion systems, solar collectors. From the point of applications, Muthucumaraswamy et al. [16] investigated the effect of unsteady flow past an exponentially accelerated infinite isothermal vertical plate with variable mass diffusion in the presence of first-order homogeneous chemical reaction. Sarma and Pandit [17] analysed the Effects of thermal radiation and chemical reaction on steady MHD mixed convective flow over a vertical porous plate with induced magnetic field. For industrial applications such as glass production, space technology applications, furnace design, spacecraft re-entry aerothermodynamics and cosmic flight aerodynamics rockets which are operated under the higher temperature with radiation effects are significant. In view of this, Suneetha et al. [18] investigated the effects of thermal radiation on the natural convective heat and mass transfer of a viscous incompressible gray absorbing-emitting fluid flowing past an impulsively started moving vertical plate with viscous dissipation. Sattar and Kalim [19] studied the unsteady free convection interaction with thermal radiation in a boundary layer flow past a vertical porous plate. Nandkeolyar et al. [20] studied the exact solutions of unsteady MHD free convection in a heat absorbing fluid flow past a flat plate with ramped wall temperature.

Most of the time Hall current was ignored in applying Ohm's law, due to the fact that it has no extraordinary effect for small and average values of the magnetic field. The effect of Hall current is very important in the presence of a strong magnetic field [21], because for strong magnetic field electromagnetic force is

prominent. When the magnetic strength is strong, Hall current cannot be neglected. The recent research for the applications of MHD is towards a strong magnetic field, due to which study of Hall current is very important. Actually, in an ionized gas where the density is low and/or the magnetic field is very strong, the conductivity normal to the magnetic field is reduced due to the free spiral movement of electrons and ions about the magnetic lines of force before suffering collisions and a current is induced in a direction normal to both electric and magnetic fields. The important engineering applications for MHD boundary layer flows with heat transfer including the effects of Hall current are encountered in MHD power generators and pumps, Hall accelerators, refrigeration coils, electric transformers, in flight MHD, solar physics involved in the sunspot development, the solar cycle, the structure of magnetic stars, electronic system cooling, cool combustors, fibre and granular insulation, oil extraction, thermal energy storage and flow through filtering devices and porous material regenerative heat exchangers.

It is noticed that when the density of an electrically conducting fluid is low and/or applied magnetic field is strong, Hall current is produced in the flow-field which plays an important role in determining flow features of the problems because it induces secondary flow in the flow-field. Keeping in view this fact, significant investigations on hydromagnetic free convection flow past a flat plate with Hall effects under different thermal conditions are carried out by several researchers in the past. Pop and Watanabe [22] analyzed the Hall effects on magneto hydrodynamic free convection about a semi-infinite vertical flat plate, Takhar et al. [23] investigated the combined effects of thermal and mass diffusion, magnetic field and Hall current on an unsteady free convection flow over an infinite vertical porous plate. Saha et al. [24] studied the effect of Hall current on MHD natural convection flow from vertical permeable flat plate with uniform surface heat flux. Satya Narayana et al. [25] studied the effects of Hall current and radiation–absorption on MHD natural convection heat and mass transfer flow of a micropolar fluid in a rotating frame of reference. Sarma and Pandit [26] investigated the effects of Hall current, rotation and Soret effects on MHD free convection heat and mass transfer flow past an accelerated vertical plate through a porous medium. Seth et al. [27] investigated effects of Hall current and rotation on unsteady hydromagnetic natural convection flow of a viscous, incompressible, electrically conducting and heat absorbing fluid past an impulsively moving vertical plate with ramped temperature in a porous medium taking into account the effects of thermal diffusion. Seth et al. [28] investigated the effects of Hall current, radiation and rotation on natural convection heat and mass transfer flow past a moving vertical plate. Takhar et al. [29] investigated the effect of hall current on MHD flow over a moving plate in a rotating fluid with magnetic field and free stream velocity. Jaber [30] analyzed the effect of Hall currents and variable fluid properties on MHD flow past stretching vertical plate in presence of radiation. Ghara et al. [31] investigated the effects of Hall Current and Ion-Slip on unsteady MHD Couette flow. Guchhait et al. [32] studied the combined effects of Hall current and radiation on MHD free convective flow in a vertical channel with an oscillatory wall temperature. Satya Narayana et al. [33] studied the effects of Hall current and radiation absorption on MHD micropolar fluid in a rotating system. Anika et al. [34] investigated the effect of Hall current on magneto hydrodynamics fluid over an infinite Rotating vertical porous plate embedded in unsteady laminar flow. Anika et al. [35] analyzed the thermal buoyancy force effects on developed flow considering Hall and Ion-slip current. Seth et al. [36] investigated the effects of Hall current on unsteady hydromagnetic free convection flow past an impulsively moving vertical plate with Newtonian heating.

The aim of the present paper is to study the effects of Hall current, rotation, chemical reaction, thermal radiation on hydromagnetic free convective heat and mass transfer flow of a viscous, incompressible, electrically conducting and heat absorbing fluid past a vertical infinite flat plate. The fluid flow is induced by a general time-dependent movement of the infinite plate. The governing equations are solved analytically, and a general solution valid for any time-dependent movement of the plate is obtained. Some particular cases that highlight the applications of the general solution are discussed. A comparison of the present solution for skin friction in the absence of Hall current, rotation, chemical reaction, thermal radiation and permeability of porous medium is made with the exact solution obtained by Nandkeolyar et al. [20]. It was found that our result is in excellent agreement with that of Nandkeolyar et al. [20].

2 Mathematical Formulation

We consider the unsteady MHD free convective heat and mass transfer flow of a viscous, incompressible, electrically conducting and heat absorbing fluid along an infinite non-conducting vertical flat plate embedded in a uniform porous medium in a rotating system taking Hall current into account. Assuming Hall currents, the generalized Ohm's law [37] may be put in the form:

$$\vec{J} = \frac{\sigma}{1+m^2}\left(\vec{E} + \vec{V}\times\vec{B} - \frac{1}{\sigma n_e}\vec{J}\times\vec{B}\right),$$

where $\vec{V}$ represents the velocity vector, $\vec{E}$ is the intensity vector of the electric field, $\vec{B}$ is the magnetic induction vector, $\vec{J}$ the electric current density vector, m is the Hall current parameter, σ the electrical conductivity and n_e is the number density of the electron. A very interesting fact that the effect of Hall current gives rise to a force in the $z'-$ direction which in turn produces a cross flow velocity in this direction and thus the flow becomes three-dimensional.

Coordinate system is chosen in such a way that x'-axis is along the plate in the upward direction, the y′-axis normal to it and the z′-axis normal to $x'y'$-plane. The fluid is permeated by a uniform transverse magnetic field of strength B0applied along the y-axis. The fluid and plate rotate in unison with uniform angular velocity Ω about y′-axis. For time $t' < 0$, the stationary plate and the fluid are at same constant temperature T'_∞ and species concentration C'_∞. At time $t' = 0$, the plate begins to move with a time-dependent velocity $U_0 f(t')$ in its own plane along the x'-axis and the temperature of the plate is raised or lowered to $T'_\infty + (T'_w - T'_\infty)t'/t_0$ when $t' < t_0$ and thereafter, for $t' > t_0$, it is maintained at a uniform temperature T'_w. Also, for time $t' > 0$, species concentration is raised to C'_w. The geometry of the problem is of infinite extent in x' and z' directions, and is electrically non-conducting, all physical quantities, except pressure, are functions of y and t' only. The fluid under consideration is a metallic liquid, such as mercury, whose magnetic Reynolds number is so small that the induced magnetic field produced by the fluid motion is negligible in comparison to the applied magnetic field $B = (0, B_0, 0)$, Cramer and Pai [21]. Also, no external electric field is applied, so the effect of polarization of the magnetic field is negligible, Meyer [38]. Under these assumptions, together with the usual boundary layer approximations, the governing equations for the unsteady MHD free convective heat and mass transfer flow of a viscous, incompressible, electrically conducting and heat absorbing fluid through a porous medium in presence of strong magnetic field are as follows:

Conservation of Momentum:

$$\frac{\partial u'}{\partial t'} + 2\Omega w' = \upsilon\frac{\partial^2 u'}{\partial y'^2} - \frac{\sigma B_0^2}{\rho(1+m^2)}(u' + mw') + g\beta(T' - T'_\infty) + g\beta'(C' - C'_\infty) - \frac{\upsilon u'}{K'_1} \quad (1)$$

$$\frac{\partial w'}{\partial t'} - 2\Omega u' = \upsilon\frac{\partial^2 w'}{\partial y'^2} + \frac{\sigma B_0^2}{\rho(1+m^2)}(mu' - w') - \frac{\upsilon w'}{K'_1} \quad (2)$$

Conservation of Energy:

$$\frac{\partial T'}{\partial t'} = \frac{k}{\rho C_p}\frac{\partial^2 T'}{\partial y'^2} - \frac{Q_0}{\rho C_p}\left(T' - T'_\infty\right) - \frac{1}{\rho C_p}\frac{\partial q_r'}{\partial y'} \tag{3}$$

Conservation of Species Concentration:

$$\frac{\partial C'}{\partial t'} = D\frac{\partial^2 C'}{\partial y'^2} - Kr'\left(C' - C'_\infty\right) \tag{4}$$

Assuming no slip condition between the plate and the fluid, the relevant initial boundary conditions are:

$$u' = 0, w' = 0, T' = T_\infty', C' = C_\infty' \text{ for } y' \geq 0 \text{ and } t' \leq 0 \tag{5a}$$

$$u' = U_0 f\left(t'\right), C' = C_w' \text{ at } y' = 0 \text{ for } t' > 0 \tag{5b}$$

$$T' = T_\infty' + \left(T_w'' - T_\infty'\right)t'/t_0 \text{ at } y' = 0 \text{ for } 0 < t' \leq t_0 \tag{5c}$$

$$T' = T_w' \text{ at } y' = 0 \text{ for } t' > t_0 \tag{5d}$$

$$u' \to 0, w' \to 0, T' \to T_\infty', C' \to C_\infty' \text{ as } y' \to \infty \text{ for } t' > 0 \tag{5e}$$

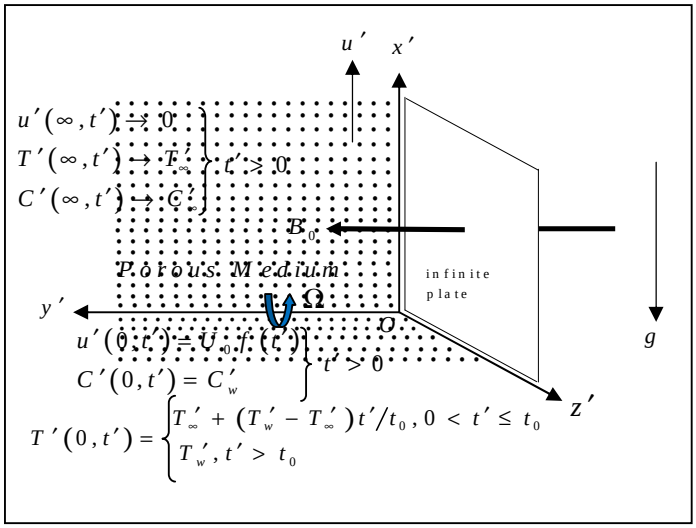

Fig. 1. Geometry of the problem

For an optically thick fluid, in addition to emission there is also self absorption and usually the absorption co-efficient is wavelength dependent and large so we can adopt the Rosseland approximation [39] for radiative heat flux vector q_r'. Thus q_r' is given by

$$q_r' = -\frac{4\sigma_1}{3k_1}\frac{\partial T'^4}{\partial y'} \tag{6}$$

where k_1 is Rosseland mean absorption co-efficient and σ_1 is Stefan-Boltzmann constant.

We assume that the temperature differences within the flow are sufficiently small so that T'^4 about the free stream temperature T_∞' and neglecting higher order terms. This results of the following approximations:

$$T'^4 \approx 4T_\infty'^3 T' - 3T_\infty'^4 \tag{7}$$

From (6) and (7) we have

$$\frac{\partial q_r'}{\partial y'} = -\frac{4\sigma_1}{3k_1}\frac{\partial^2 T'^4}{\partial y'^2} = -\frac{16\sigma_1 T_\infty'^3}{3k_1}\frac{\partial^2 T'}{\partial y'^2} \tag{8}$$

Thus the energy equation (3) reduces to

$$\frac{\partial T'}{\partial t'} = \frac{k}{\rho C_p}\frac{\partial^2 T'}{\partial y'^2} - \frac{Q_0}{\rho C_p}\left(T' - T_\infty'\right) + \frac{16\sigma_1 T_\infty'^3}{3k_1\rho C_p}\frac{\partial^2 T'}{\partial y'^2} \tag{9}$$

Introducing the following non-dimensional quantities:

$$y = \frac{y'}{U_0 t_0}, u = \frac{u'}{U_0}, w = \frac{w'}{U_0}, t = \frac{t'}{t_0}, \theta = \frac{T' - T_\infty'}{T_w' - T_\infty'}, \phi = \frac{C' - C_\infty'}{C_w' - C_\infty'}, Gr = \frac{g\beta\upsilon\left(T_w' - T'\right)}{U_0^3},$$
$$Gm = \frac{g\beta'\upsilon\left(C_w' - C_\infty'\right)}{U_0^3}, M^2 = \frac{\sigma B_0^2\upsilon}{\rho U_0^2}, \Pr = \frac{\mu Cp}{k}, Sc = \frac{\upsilon}{D}, Q = \frac{\upsilon Q_0}{\rho Cp U_0^2}, t_0 = \frac{\upsilon}{U_0^2},$$
$$K_1 = \frac{K_1' U_0^2}{\upsilon^2}, N = \frac{kk_1}{4\sigma_1 T_\infty'^3}, \lambda = \frac{3N+4}{3N}, Kr = \frac{\upsilon Kr'}{U_0^2}, K^2 = \frac{\upsilon\Omega}{U_0^2}.$$

Equation (1)-(3) and (9) reduces to

$$\frac{\partial u}{\partial t} + 2K^2 w = \frac{\partial^2 u}{\partial y^2} - \frac{M^2}{\left(1+m^2\right)}\left(u + mw\right) + Gr\theta + Gm\phi - \frac{u}{K_1} \tag{10}$$

$$\frac{\partial w}{\partial t} - 2K^2 u = \frac{\partial^2 w}{\partial y^2} + \frac{M^2}{\left(1+m^2\right)}\left(mu - w\right) - \frac{w}{K_1} \tag{11}$$

$$\frac{\partial \theta}{\partial t} = \frac{\lambda}{\Pr}\frac{\partial^2 \theta}{\partial y^2} - Q\theta \tag{12}$$

$$\frac{\partial \phi}{\partial t} = \frac{1}{Sc}\frac{\partial^2 \phi}{\partial y^2} - Kr\phi \tag{13}$$

The corresponding initial and boundary conditions in non-dimensional form become:

$$u = 0, w = 0, \theta = 0, \phi = 0 \text{ for } y \geq 0 \text{ and } t \leq 0 \tag{14a}$$

$$u = f(t), \phi = 1 \text{ at } y = 0 \text{ for } t > 0 \tag{14b}$$

$$\theta = t \text{ at } y = 0 \text{ for } 0 < t \leq 1 \tag{14c}$$

$$\theta = 1 \text{ at } y = 0 \text{ for } t > 1 \tag{14d}$$

$$u \to 0, w \to 0, \theta \to 0, \phi \to 0 \text{ as } y \to \infty \text{ for } t > 0 \tag{14e}$$

Equations (10) and (11) are presented, in compact form, as

$$\frac{\partial F}{\partial t} = \frac{\partial^2 F}{\partial y^2} - \alpha F + Gr\theta + Gm\phi \tag{15}$$

where, $F = u + iw$ and $\alpha = M^2(1 - im)/(1 + m^2) + 1/K_1 - 2iK^2$

The initial and boundary conditions (14a)-(14e), in compact form, become

$$F = 0, \theta = 0, \phi = 0 \text{ for } y \geq 0 \text{ and } t \leq 0 \tag{16a}$$

$$F = f(t), \phi = 1 \text{ at } y = 0 \text{ for } t > 0 \tag{16b}$$

$$\theta = t \text{ at } y = 0 \text{ for } 0 < t \leq 1 \tag{16c}$$

$$\theta = 1 \text{ at } y = 0 \text{ for } t > 1 \tag{16d}$$

$$F \to 0, \theta \to 0, \phi \to 0 \text{ as } y \to \infty \text{ for } t > 0 \tag{16e}$$

The system of differential equations (12), (13) and (15) together with the initial and boundary conditions (16a)-(16e) describes our model for the MHD free convective heat and mass transfer flow of a viscous, incompressible, electrically conducting and heat absorbing fluid past an infinite vertical plate embedded in a porous medium with ramped wall temperature taking Hall current and rotation into consideration.

3 Solution of the Problem

The set of equations (12), (13) and (15) subject to the initial and boundary conditions (16a)-(16e) were solved analytically using Laplace transforms. The exact solutions for species concentration $\phi(y, t)$, fluid temperature $\theta(y, t)$ and fluid velocity $F(y, t)$ are respectively,

$$\phi(y,t)=\frac{1}{2}\left[e^{y\sqrt{ScKr}}erfc\left(\frac{y}{2}\sqrt{\frac{Sc}{t}}+\sqrt{Krt}\right)+e^{-y\sqrt{ScKr}}erfc\left(\frac{y}{2}\sqrt{\frac{Sc}{t}}-\sqrt{Krt}\right)\right] \tag{17}$$

$$\theta(y,t)=\theta_1(y,t)-H(t-1)\theta_1(y,t-1) \tag{18}$$

$$F(y,t)=P(y,t)+\alpha_1\left[P_1(y,t)-H(t-1)P_1(y,t-1)\right]+\alpha_2P_2(y,t) \tag{19}$$

where, $P(y,t)=L^{-1}\left\{\overline{f}(s)e^{-y\sqrt{s+A_1}}\right\}$

Here, $H(t-1)$, $erfc(x)$ and L^{-1} are Heaviside unit step function, the complimentary error function and the inverse Laplace transform operator respectively.

4.1 Solution in the case of isothermal plate

Equations (17)-(19) represent the analytical solutions for species concentration, fluid temperature and fluid velocity for free convection heat and mass transfer flow of a viscous, incompressible, electrically conducting and heat absorbing fluid past a flat plate through porous medium with ramped temperature taking Hall current and rotation into account. In order to highlight the effects of the ramped temperature distribution on the fluid flow, it is worthwhile to compare such a flow with the flow near a moving plate with constant temperature. The solution for species concentration is given by equation (17). However, the fluid temperature and velocity for free convection near an isothermal plate has the following form:

$$\theta(y,t)=\frac{1}{2}\left[e^{y\sqrt{\frac{\Pr Q}{\lambda}}}erfc\left(\frac{y}{2}\sqrt{\frac{\Pr}{\lambda t}}+\sqrt{Qt}\right)+e^{-y\sqrt{\frac{\Pr Q}{\lambda}}}erfc\left(\frac{y}{2}\sqrt{\frac{\Pr}{\lambda t}}-\sqrt{Qt}\right)\right] \tag{20}$$

$$F(y,t)=P(y,t)+\alpha_1P_3(y,t)+\alpha_2P_2(y,t) \tag{21}$$

4.2 Sherwood number

The Sherwood number *Sh*, which measures the rate of mass transfer at the plate, is given by

$$Sh=-\left(\frac{\partial\phi}{\partial y}\right)_{y=0}=\sqrt{ScKr}erf\left(\sqrt{Krt}\right)+\sqrt{\frac{Sc}{\pi t}}e^{-Krt} \tag{22}$$

4.3 Nusselt number

The Nusselt number *Nu*, which measures the rate of heat transfer at the plate, and for a ramped temperature plate it is given by

$$Nu=-\left(\frac{\partial\theta}{\partial y}\right)_{y=0}=-\left[\theta_2(0,t)-H(t-1)\theta_2(0,t-1)\right] \tag{23}$$

In case of an isothermal plate, the Nusselt number is given by

$$Nu_i = \sqrt{\frac{\Pr Q}{\lambda}} erf\left(\sqrt{Qt}\right) + \sqrt{\frac{\Pr}{\pi\lambda t}} e^{-Qt} \tag{24}$$

Equations (17)-(21) represent the analytical solutions for the flow due to time-dependent movement of the vertical flat plate through porous medium. In order get some physical understanding of the flow behaviour, some particular cases of time-dependent movements of the plate are discussed below.

4.4 Plate moving with uniform velocity

Let us consider that the plate moving with a uniform velocity $f(t) = H(t)$, the fluid velocity of the flow for the ramped temperature plate is obtained as

$$F(y,t) = P_4(y,t) + \alpha_1\left[P_1(y,t) - H(t-1)P_1(y,t-1)\right] + \alpha_2 P_2(y,t) \tag{25}$$

and for the isothermal plate the fluid velocity is

$$F(y,t) = P_4(y,t) + \alpha_1 P_3(y,t) + \alpha_2 P_2(y,t) \tag{26}$$

The expression for the skin friction for the ramped temperature plate is given by

$$\tau_{1x} + i\tau_{1z} = \left(\frac{\partial F}{\partial y}\right)_{y=0} = Q_1(t) + \alpha_1\left[F_1(t) - H(t-1)F_1(t-1)\right] + \alpha_2 F_2(t) \tag{27}$$

and for the isothermal plate it is given by

$$\tau'_{1x} + \tau'_{1z} = Q_1(t) + \alpha_1 F_3(t) + \alpha_2 F_2(t) \tag{28}$$

4.5 Plate moving with uniform acceleration

Let us consider that the plate is moving with uniform acceleration $f(t) = tH(t)$, the fluid velocity of the flow for the ramped temperature plate is obtained as

$$F(y,t) = P_5(y,t) + \alpha_1\left[P_1(y,t) - H(t-1)P_1(y,t-1)\right] + \alpha_2 P_2(y,t) \tag{29}$$

and for the isothermal plate the fluid velocity is

$$F(y,t) = P_5(y,t) + \alpha_1 P_3(y,t) + \alpha_2 P_2(y,t) \tag{30}$$

The expression for the skin friction for the ramped temperature plate is given by

$$\tau_{2x} + i\tau_{2z} = \left(\frac{\partial F}{\partial y}\right)_{y=0} = Q_2(t) + \alpha_1\left[F_1(t) - H(t-1)F_1(t-1)\right] + \alpha_2 F_2(t) \tag{31}$$

and for the isothermal plate it is given by

$$\tau'_{2x} + i\tau'_{2z} = Q_2(t) + \alpha_1 F_3(t) + \alpha_2 F_2(t) \tag{32}$$

4.6 Plate moving with periodic acceleration

Let us consider that the plate is moving with periodic acceleration $f(t) = \cos \omega t H(t)$, the fluid velocity of the flow for the ramped temperature plate is obtained as

$$F(y,t) = P_6(y,t) + \alpha_1 \left[P_1(y,t) - H(t-1) P_1(y,t-1) \right] + \alpha_2 P_2(y,t) \tag{33}$$

and for the isothermal plate the fluid velocity is

$$F(y,t) = P_6(y,t) + \alpha_1 P_3(y,t) + \alpha_2 P_2(y,t) \tag{34}$$

The expression for the skin friction for the ramped temperature plate is given by

$$\tau_{3x} + i\tau_{3z} = \left(\frac{\partial F}{\partial y} \right)_{y=0} = Q_3(t) + \alpha_1 \left[F_1(t) - H(t-1) F_1(t-1) \right] + \alpha_2 F_2(t) \tag{35}$$

and for the isothermal plate it is given by

$$\tau'_{3x} + i\tau'_{3z} = Q_3(t) + \alpha_1 F_3(t) + \alpha_2 F_2(t) \tag{36}$$

5 Results and Discussion

In order to get the physical understanding of the problem and for the purpose of analyzing the effect of Hall current, rotation, chemical reaction, thermal radiation, concentration buoyancy force, thermal buoyancy force, thermal diffusion, mass diffusion, permeability of porous medium and time on the flow field, numerical values of the primary and secondary fluid velocities, fluid temperature and species concentration in the boundary layer region were computed for both ramped temperature and isothermal plate, in all three cases and are displayed graphically versus boundary layer co-ordinate y in Figs. 2-12 for various values of thermal Grashof number (*Gr*), solutal Grashof number (*Gm*), Hall current parameter (*m*), rotation parameter (K^2), Schmidt number (*Sc*), permeability parameter (K_1), chemical reaction parameter (*Kr*), thermal radiation parameter (*N*) and time (*t*) taking magnetic parameter M^2=3 and $\omega = \pi/2$. The numerical values of skin friction, heat transfer co-efficient in terms of Nusselt number (*Nu*) and mass transfer co-efficient in terms of Sherwood number (*Sh*) are depicted in Tables 1-19 for both ramped temperature and isothermal plate. During the course of numerical calculations of the fluid velocity, the temperature and the species concentration, the values of the Prandtl number are chosen for mercury (*Pr*=0.025), air at 25^oC and one atmospheric pressure (*Pr*=0.71), electrolytic solution (*Pr*=1.0) and water (*Pr*=7.0). To focus our attention on numerical values of the results obtained in the study, the values of *Sc* are chosen for the gases representing diffusing chemical species of most common interest in air, namely, hydrogen (*Sc*=0.22), water-vapour (*Sc*=0.60) and ammonia (*Sc*=0.78). To examine the effect of parameters related to the problem on the velocity field, the skin friction numerical computation are carried out at *Pr*=0.71 and *Sc*=0.60. To find solution of this problem, we have placed an infinite vertical plate in a finite length in the flow. Hence, we solve the entire problem in a finite boundary.

Fig. 2 shows that for both ramped temperature and isothermal plates, the primary and secondary fluid velocities u(y, t) and w(y, t) increases with an increase in time t for all cases except in the case of periodic

acceleration of the plate. In this case, both primary and secondary fluid velocities decrease with an increase in time t. Figs. 3-4 depict the influence of thermal and concentration buoyancy forces on the primary and secondary fluid velocities for both ramped temperature and isothermal plate in all three cases. It is revealed from Figs. 3-4 that the primary velocity u(y, t) increases asymptotically on increasing *Gr* and *Gm* throughout the boundary layer region, whereas the secondary fluid velocity w(y, t) increases on increasing *Gr* and *Gm* in a region near to the surface of the plate and it decreases on increasing *Gr* and *Gm* in the region away from the plate. *Gr* represents the relative strength of thermal buoyancy force to viscous force and Gm represents the relative strength of concentration buoyancy force to viscous force. Therefore, *Gr* increases on increasing the strengths of thermal buoyancy force whereas Gm increases on increasing the strength of concentration buoyancy force. In this problem, natural convection flow induced due to thermal and concentration buoyancy forces, therefore, thermal and concentration buoyancy force tends to accelerate the fluid velocity throughout the boundary layer region which is clearly evident from Figs. 3-4. Fig. 5 demonstrates the effect of Hall current (*m*) on primary and secondary velocities for both ramped temperature and isothermal plate, in all three cases. It is perceived from Fig. 5 that, the primary velocity u(y, t) increases on increasing m in a region near to the surface of the plate but it starts decreasing on increasing m in the region away from the plate whereas secondary fluid velocity w(y, t) increases on increasing m throughout the boundary layer region. This implies that, Hall current tends to accelerate secondary fluid velocity throughout the boundary layer region which is consistent with the fact that Hall current induces secondary flow in the flow-field whereas it has a reverse effect on primary fluid velocity. Fig. 6 illustrates the effect of rotation (K^2) on the primary and secondary fluid velocities for both ramped temperature and isothermal plate, in all three cases. It is evident from Fig. 6 that, primary velocity u(y, t) decreases on increasing K^2 whereas secondary fluid velocity w(y, t) increases on increasing K^2 in the region away from the plate. This implies that rotation retards fluid flow in the primary flow direction and accelerates fluid flow in the secondary flow direction in the boundary layer region. This may be attributed to the fact that when the frictional layer at the moving plate is suddenly set into the motion then the coriolis force acts as a constraint in the main fluid flow i.e., in the fluid flow in the primary flow direction to generate cross flow i.e., secondary flow. The influence of the Schmidt number (*Sc*) on the primary and secondary fluid velocities and concentration profiles are plotted in Figs. 7 and 12(a) respectively. It is noticed from Figs. 7 and 12(a) that, u(y, t), w(y, t) for both ramped temperature and isothermal plate and concentration ϕ decreases on increasing *Sc*. The Schmidt number embodies the ratio of the momentum to the mass diffusivity. The Schmidt number therefore quantifies the relative effectiveness of momentum to mass transport by diffusion in the hydrodynamic (velocity) and concentration (species) boundary layers. As the Schmidt number increases the concentration decreases. This cause the concentration buoyancy effects to decrease yielding a reduction in the fluid velocity. The reductions in the velocity and concentration profiles are accompanied by simultaneous reductions in the velocity and concentration boundary layers. These behaviours are clear from Figs. 7 and 12(a).

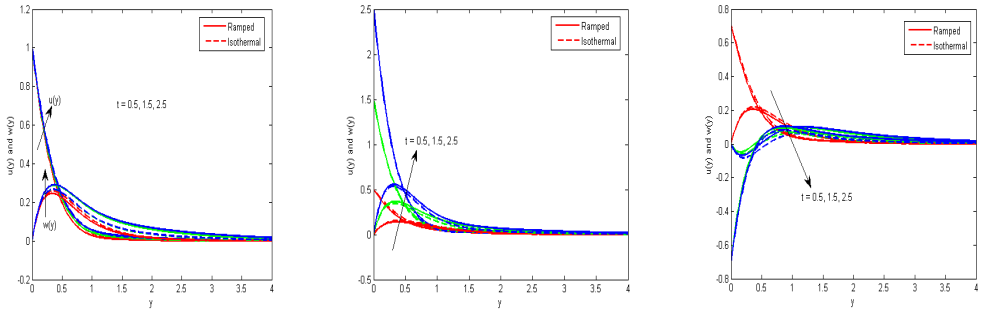

(a) (b) (c)

Fig. 2. Effect of variation in time *t* on the fluid velocities $u(y,t)$ and $w(y,t)$ when (a) $f(t)=H(t)$, (b) $f(t)=tH(t)$ and (c) $f(t)=\cos\omega t H(t)$

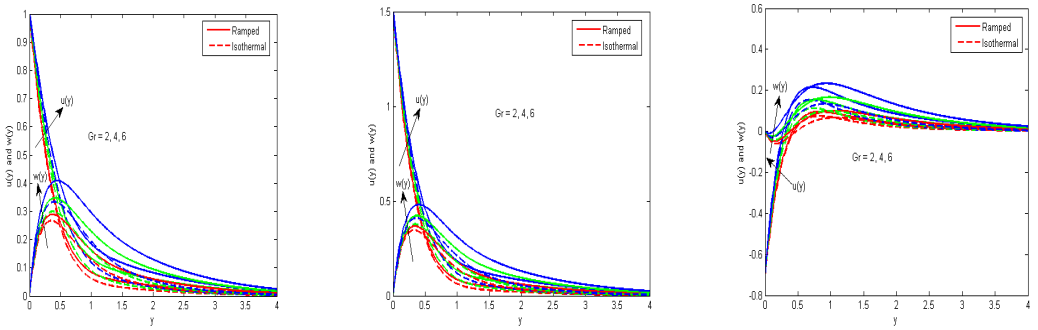

(a) **(b)** **(c)**

Fig. 3. Effect of variation in thermal Garashof number *Gr* on the fluid velocities $u(y,t)$ and $w(y,t)$ when

(a) $f(t)=H(t)$, **(b)** $f(t)=tH(t)$ **and (c)** $f(t)=\cos\omega tH(t)$

Fig. 8 demonstrates the influence of chemical reaction parameter (*Kr*) on the primary and secondary fluid velocities for both ramp temperature and isothermal plate, in all three cases. As can be seen, an increase in the chemical reaction parameter (*Kr*) leads to decrease in the thickness of the velocity boundary layer; this shows that diffusion rate can be tremendously altered by chemical reaction. It should be mentioned here that physically positive values of *Kr* implies destructive reaction and negative values of *Kr* implies generative reaction. We studied the case of a destructive chemical reaction. Fig. 9 presents the effect of thermal radiation (*N*) on the primary and secondary fluid velocities for both ramp temperature and isothermal plate, in all three cases. It is evident from Fig. 9 that u(y, t) and w(y, t) decreases on increasing *N* for ramped temperature whereas for isothermal plate u(y, t) and w(y, t) increases on increasing *N*. This implies that thermal radiation tends to retard the primary and secondary fluid velocities for ramped temperature, whereas, it has reverse effect for isothermal plate. Fig. 10 presents the effect of permeability of porous medium (K_1) on the primary and secondary fluid velocities for both ramp temperature and isothermal plate, in all three cases. It is noticed from Fig. 10 that primary fluid velocity u(y, t) decreases on increasing permeability parameter whereas it has reverse effect on secondary fluid velocity w(y, t). From the flow configuration it is obvious that an increase in porosity of the medium assist the flow along the secondary direction thereby causing the secondary fluid velocity to increase due to its orientation through the porous medium.

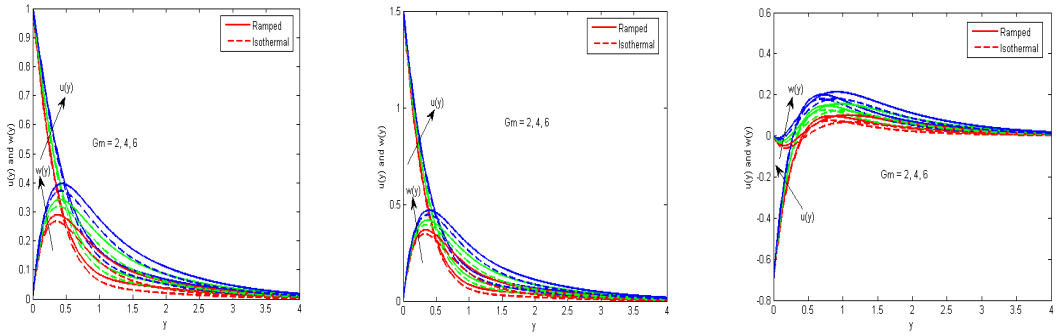

(a) **(b)** **(c)**

Fig. 4. Effect of variation in solutal Garashof number *Gm* on the fluid velocities $u(y,t)$ and $w(y,t)$ when

(a) $f(t)=H(t)$, **(b)** $f(t)=tH(t)$ **and (c)** $f(t)=\cos\omega tH(t)$

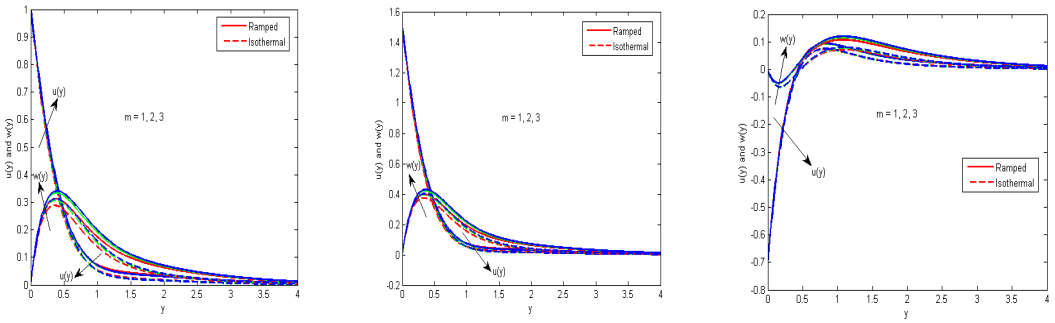

(a) **(b)** **(c)**

Fig. 5. Effect of variation in *m* on the fluid velocities $u(y,t)$ and $w(y,t)$ when (a) $f(t)=H(t)$, (b) $f(t)=tH(t)$ and (c) $f(t)=\cos\omega t H(t)$

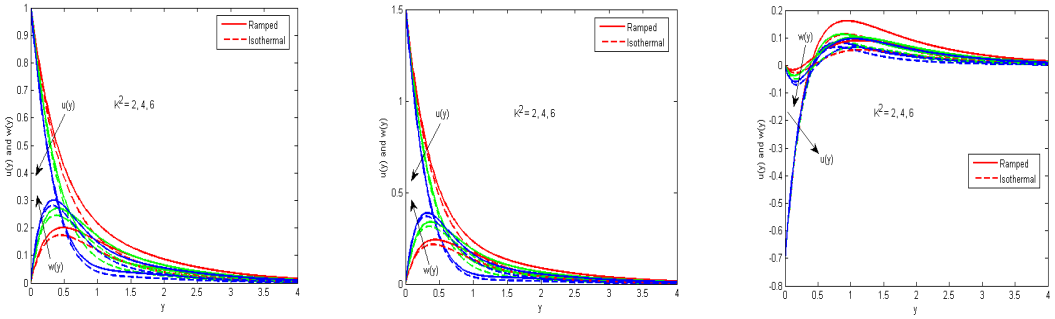

(a) **(b)** **(c)**

Fig. 6. Effect of variation in K^2 on the fluid velocities $u(y,t)$ and $w(y,t)$ when (a) $f(t)=H(t)$, (b) $f(t)=tH(t)$ and (c) $f(t)=\cos\omega t H(t)$

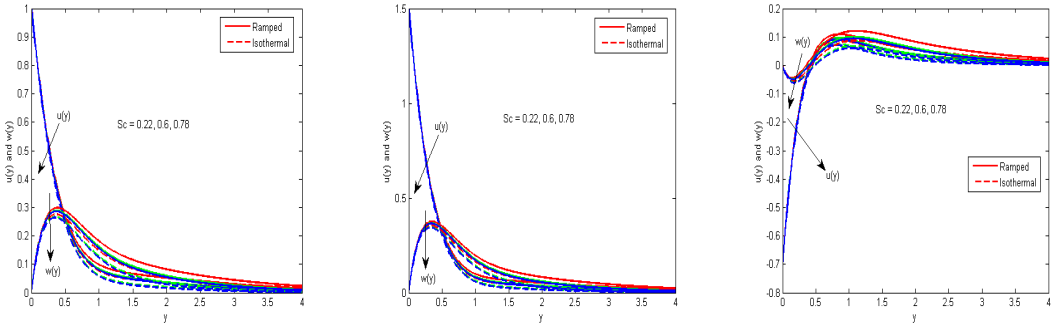

(a) **(b)** **(c)**

Fig. 7. Effect of variation in Schmidt number *Sc* on the fluid velocities $u(y,t)$ and $w(y,t)$ when (a) $f(t)=H(t)$, (b) $f(t)=tH(t)$ and (c) $f(t)=\cos\omega t H(t)$

The numerical values of fluid temperature θ, computed from the analytic solutions (18) and (20), are displayed graphically versus boundary layer co-ordinate y in Fig. 11 for various values of Prandtl number *Pr*, thermal radiation and time *t*. It is evident from Fig. 11(a) that, fluid temperature θ decreases on increasing *Pr*. An increase in Prandtl number reduces the thermal boundary layer thickness. Prandtl number signifies the

ratio of momentum diffusivity to thermal diffusivity. It can be noticed that as *Pr* decreases, the thickness of the thermal boundary layer becomes greater than the thickness of the velocity boundary layer according to the well-known relation $\delta T/\delta \cong 1/\Pr$ where δT the thickness of the thermal boundary layer and δ the thickness of the velocity boundary layer, so the thickness of the thermal boundary layer increases as Prandtl number decreases and hence temperature profile decreases with increase in Prandtl number. In heat transfer problems, the Prandtl number controls the relative thickening of momentum and thermal boundary layers.

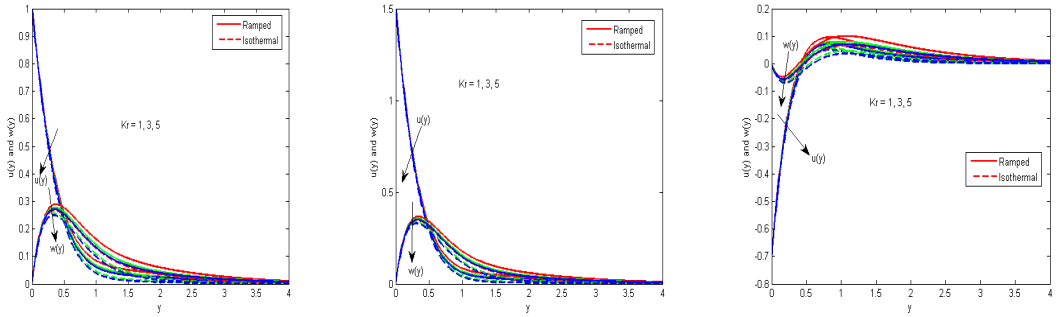

(a) **(b)** **(c)**

Fig. 8. Effect of variation in *Kr* on the fluid velocities $u(y,t)$ and $w(y,t)$ when (a) $f(t)=H(t)$, (b) $f(t)=tH(t)$ and (c) $f(t)=\cos\omega tH(t)$

When Prandtl number is small, it means that heat diffuses quickly compared to the velocity (momentum), which means that for liquid metals, the thickness of the thermal boundary layer is much bigger than the momentum boundary layer. Hence Prandtl number can be used to increase the rate of cooling in conducting flows. Fig. 11(b) is plotted to depict the influence of the thermal radiation parameter *N* on the temperature profile. We observe in this figure that increasing thermal radiation parameter produces a significant decrease in the thermal condition of the fluid flow for ramped temperature, whereas, it has reverse effect for isothermal plate. This can be explained by the fact that a decrease in the values of radiation parameter $N=kk_1/4\sigma_1 T_\infty'^3$ means a decrease in the Rosseland radiation absorptivity k_1. Thus the divergence of the radiative heat flux decreases as k_1 increases the rate of radiative heat transferred from the fluid and consequently the fluid temperature decreases for ramp temperature. Fig. 11(c) shows that fluid temperature θ increases on increasing time *t* for both ramped temperature and isothermal plate. This implies that, there is an enhancement in fluid temperature with the progress of time throughout the thermal boundary layer region.

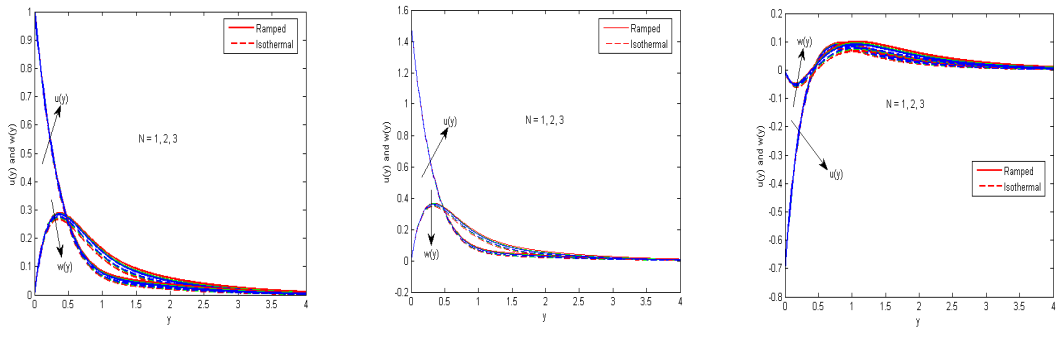

(a) **(b)** **(c)**

Fig. 9. Effect of variation in *N* on the fluid velocities $u(y,t)$ and $w(y,t)$ when (a) $f(t)=H(t)$, (b) $f(t)=tH(t)$ and (c) $f(t)=\cos\omega tH(t)$

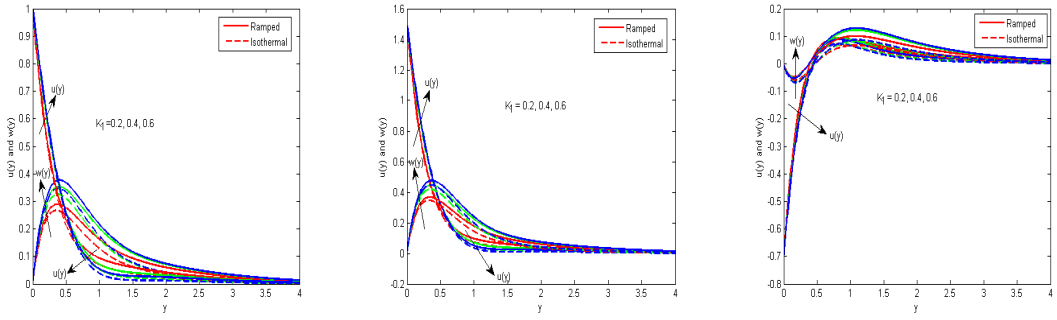

(a) **(b)** **(c)**

Fig. 10. Effect of variation in K_1 on the fluid velocities $u(y,t)$ and $w(y,t)$ when (a) $f(t)=H(t)$, (b) $f(t)=tH(t)$ and (c) $f(t)=\cos\omega t H(t)$

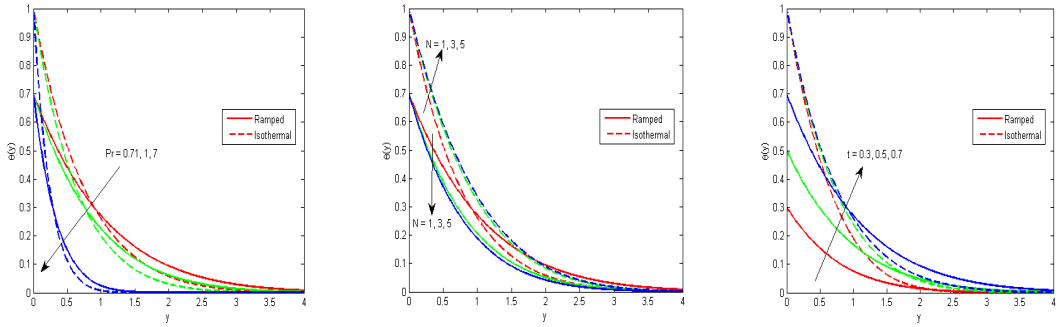

(a) (b) (c)

Fig. 11. Effect of variation in (a) the Prandtl number *Pr* (b) the radiation parameter *N*, and (c) time *t* on $\theta(y,t)$

The numerical values of species concentration ϕ, computed from the analytical solution (17), are depicted graphically versus boundary layer co-ordinate y in Figs. 12 for various values of Schmidt number *Sc*, chemical reaction parameter *Kr* and time *t*. It is noticed from Fig. 12(b) that concentration distributions decrease when the chemical reaction increases for both ramped temperature and isothermal plate. Here, we are analyzing the effects of a destructive chemical reaction (*Kr*>0). Physically, for a destructive case, chemical reaction takes place with many disturbances. This, in turn, causes high molecular motion, which results in an increase in the transport phenomenon, thereby reducing the concentration distributions in the fluid flow. From Fig. 12(c), it is clear that with unabated mass diffusion into the fluid stream, the molar concentration of the mixture rises with increasing time and so there is an enhancement in species concentration with the progress of time throughout the boundary layer region.

Table 1. Skin Friction for ramped temperature plate for different values of *m* and K^2

$m\downarrow K^2\rightarrow$	$-\tau_{1x}$			τ_{1z}		
	3	**5**	**7**	**3**	**5**	**7**
0.5	3.4334	3.6696	3.9001	1.1708	1.6461	2.0589
1	3.3361	3.5895	3.8307	1.2658	1.7326	2.1405
1.5	3.2545	3.5200	3.7682	1.2901	1.7560	2.1643

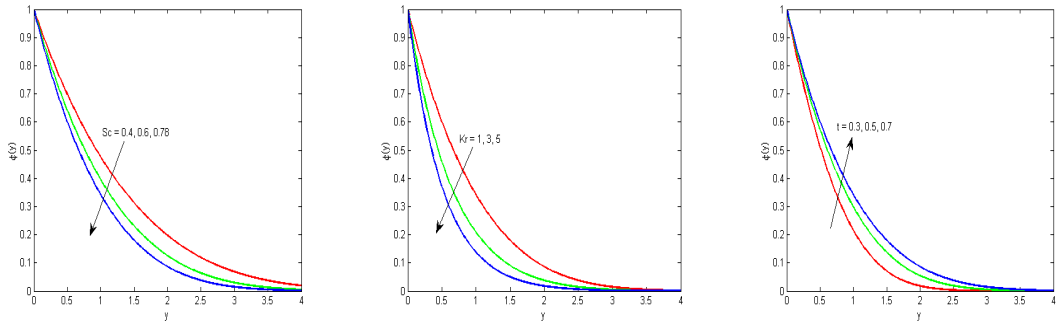

(a) (b) (c)

Fig. 12. Effect of variation in (a) the Schmidt number *Sc* (b) the chemical reaction parameter *Kr*, and (c) time *t* on $\phi(y,t)$

The numerical values of primary skin friction τ_x and secondary skin friction τ_z, computed from analytical expressions (27), (28), (31), (32), (35) and (36), are presented in tabular form for various values of *m*, K^2, *Pr*, *Sc*, *N* and *t* in Tables 1-6 for plate moving with uniform velocity, Tables 7-12 for plate moving with uniform acceleration and Tables 13-18 for plate moving with periodic acceleration respectively, taking M^2=3 and K_1=0.6. It is evident from Tables 1-6 that for plate moving with uniform velocity, primary skin friction τ_{1x} decreases on increasing *m* and *Sc* whereas it increases on increasing K^2, *Pr*,

Table 2. Skin Friction for isothermal plate for different values of *m* and K^2

$m\downarrow K^2\rightarrow$	$-\tau_{1x}$			τ_{1z}		
	3	**5**	**7**	**3**	**5**	**7**
0.5	3.3732	3.6137	3.8495	1.1832	1.6638	2.0789
1	3.2748	3.5332	3.7801	1.2792	1.7521	2.1614
1.5	3.1923	3.4628	3.7176	1.3037	1.7766	2.1857

Table 3. Skin Friction for ramped temperature plate for different values of *Pr* and *Sc*

$Pr\downarrow Sc\rightarrow$	$-\tau_{1x}$			τ_{1z}		
	0.22	**0.6**	**0.78**	**0.22**	**0.6**	**0.78**
0.025	3.3841	3.2885	3.2636	1.8086	1.8804	1.8922
0.71	3.4933	3.3978	3.3720	1.7494	1.8026	1.8048
1	3.5334	3.4352	3.4065	1.7251	1.7744	1.7762

Table 4. Skin Friction for isothermal plate for different values of *Pr* and *Sc*

$Pr\downarrow Sc\rightarrow$	$-\tau_{1x}$			τ_{1z}		
	0.22	**0.6**	**0.78**	**0.22**	**0.6**	**0.78**
0.025	3.219	3.3959	3.4626	1.8866	1.7832	1.7403
0.71	3.4374	3.6137	3.6804	1.7672	1.6638	1.6209
1	3.4999	3.6762	3.7429	1.7305	1.6271	1.5842

Table 5. Skin Friction for ramped temperature plate for different values of *N* and *t*

$N\downarrow t\rightarrow$	$-\tau_{1x}$			τ_{1z}		
	0.5	**1.5**	**2.5**	**0.5**	**1.5**	**2.5**
1	3.5967	3.6696	3.6822	1.6767	1.6461	1.6377
3	3.6748	3.7510	3.7572	1.6304	1.5974	1.5926
5	3.6996	3.7772	3.7812	1.6146	1.5808	1.5774

Table 6. Skin Friction for isothermal plate for different values of *N* and *t*

$N\downarrow t\rightarrow$	$-\tau_{1x}$			τ_{1z}		
	0.5	**1.5**	**2.5**	**0.5**	**1.5**	**2.5**
1	3.5046	3.6137	3.6630	1.7095	1.6638	1.6449
3	3.5406	3.6764	3.7319	1.6822	1.6262	1.6035
5	3.5565	3.6964	3.7538	1.6746	1.6137	1.5896

Table 7. Skin Friction for ramped temperature plate for different values of *m* and K^2

$m\downarrow K^2\rightarrow$	$-\tau_{2x}$			τ_{2z}		
	3	**5**	**7**	**3**	**5**	**7**
0.5	5.0661	5.4032	5.7462	1.7169	2.4492	3.0845
1	4.9133	5.2779	5.6391	1.8541	2.5791	3.2080
1.5	4.7880	5.1705	5.5434	1.8853	2.6130	3.2437

Table 8. Skin Friction for isothermal plate for different values of *m* and K^2

$m\downarrow K^2\rightarrow$	$-\tau_{2x}$			τ_{2z}		
	3	**5**	**7**	**3**	**5**	**7**
0.5	5.0058	5.3473	5.6957	1.7293	2.4670	3.1045
1	4.8520	5.2216	5.5886	1.8676	2.5986	3.2290
1.5	4.7258	5.1133	5.4927	1.8990	2.6336	3.2651

Table 9. Skin Friction for ramped temperature plate for different values of *Pr* and *Sc*

$Pr\downarrow Sc\rightarrow$	$-\tau_{2x}$			τ_{2z}		
	0.22	**0.6**	**0.78**	**0.22**	**0.6**	**0.78**
0.025	5.1177	5.2940	5.3607	2.6117	2.5083	2.4654
0.71	5.2269	5.4032	5.4699	2.5525	2.4492	2.4062
1	5.2669	5.4432	5.5099	2.5282	2.4249	2.3819

Table 10. Skin Friction for isothermal plate for different values of *Pr* and *Sc*

$Pr\downarrow Sc\rightarrow$	$-\tau_{2x}$			τ_{2z}		
	0.22	**0.6**	**0.78**	**0.22**	**0.6**	**0.78**
0.025	4.9532	5.1295	5.1962	2.6897	2.5863	2.5434
0.71	5.1710	5.3473	5.4140	2.5703	2.4670	2.4240
1	5.2334	5.4097	5.4764	2.5336	2.4303	2.3873

Table 11. Skin Friction for ramped temperature plate for different values of *N* and *t*

$N\downarrow t\rightarrow$	$-\tau_{2x}$			τ_{2z}		
	0.5	**1.5**	**2.5**	**0.5**	**1.5**	**2.5**
1	2.0978	5.4032	8.6425	0.7392	2.4492	4.1763
3	2.1758	5.4846	8.7175	0.6929	2.4005	4.1312
5	2.2006	5.5108	8.7415	0.6771	2.3839	4.1160

Table12. Skin Friction for isothermal plate for different values of *N* and *t*

$N\downarrow t\rightarrow$	$-\tau_{2x}$			τ_{2z}		
	0.5	**1.5**	**2.5**	**0.5**	**1.5**	**2.5**
1	2.0056	5.3473	8.6233	0.7721	2.4670	4.1835
3	2.0417	5.4099	8.6922	0.7448	2.4293	4.1421
5	2.0576	5.4299	8.7141	0.7371	2.4168	4.1282

N and *t* for both ramped temperature and isothermal plates. Secondary skin friction τ_{1z} decreases on increasing *Pr*, *N* and *t* whereas it increases on increasing *m*, K^2 and *Sc* for both ramped temperature and isothermal plate. It is evident from Tables 7-12 that for plate moving with uniform acceleration, primary skin friction τ_{2x} decreases on increasing *m* whereas it increases on increasing K^2, *Pr*, *Sc*, *N* and *t* for both ramped temperature and isothermal plates. Secondary skin friction τ_{2z} decreases on increasing *Pr*, *Sc* and *N* whereas it increases on increasing *m*, K^2 and *t* for both ramped temperature and isothermal plate. It is evident from Tables 13-18 that for plate moving with periodic acceleration, primary skin friction τ_{3x} decreases on increasing *m*, *Pr*, *Sc*, *N* and *t* whereas it increases on increasing K^2 for both ramped temperature and isothermal plates. Secondary skin friction τ_{3z} increases on increasing *m*, K^2, *Pr*, *Sc*, *N* and *t* for both ramped temperature and isothermal plate. Table 19 illustrate the influence of different physical parameters *Pr*, *N*, *Sc*, *Kr* and *t* on Nusselt number and Sherwood number. It is evident from Table 19 that Nusselt number for both ramp temperature and isothermal plate increases with *Pr* and *t*, which implies that time has a tendency to enhance the rate of heat transfer at the plate, whereas thermal radiation has the reverse effect on it. It is also observed from Table 19 that the Sherwood number increases with an increase in *Sc* and *Kr*, whereas it decreases with an increase in time *t*. Thus both mass diffusivity and time tend to reduce the rate of mass transfer at the plate. Tables 20, 21 and 22 shows the comparison of present solution for skin friction for plate moving with different velocities with Nandkeolyar et al. [20] in the absence of Hall current, rotation, chemical reaction, thermal radiation and permeability of porous medium is made with the exact solution obtained by Nandkeolyar [20]. It was found that our result is in excellent agreement with that of Nandkeolyar [20].

Table 13. Skin Friction for ramped temperature plate for different values of *m* and K^2

$m\downarrow K^2\rightarrow$	τ_{3x}			$-\tau_{3z}$		
	3	**5**	**7**	**3**	**5**	**7**
0.5	1.8116	1.9729	2.1654	0.8230	1.2405	1.5881
1	1.7187	1.9017	2.1094	0.8887	1.3128	1.6569
1.5	1.6458	1.8403	2.0581	0.8973	1.3321	1.6782

Table14. Skin Friction for isothermal plate for different values of *m* and K^2

$m\downarrow K^2\rightarrow$	τ_{3x}			$-\tau_{3z}$		
	3	**5**	**7**	**3**	**5**	**7**
0.5	1.8718	2.0288	2.2159	0.8106	1.2228	1.5681
1	1.7800	1.9581	2.1599	0.8752	1.2933	1.6360
1.5	1.7080	1.8975	2.1088	0.8837	1.3115	1.6568

Table15. Skin Friction for ramped temperature plate for different values of *Pr* and *Sc*

$Pr\downarrow Sc\rightarrow$	τ_{3x}			$-\tau_{3z}$		
	0.22	**0.6**	**0.78**	**0.22**	**0.6**	**0.78**
0.025	2.2584	2.0821	2.0154	1.0781	1.1814	1.2243
0.71	2.1492	1.9062	1.9729	1.1372	1.2405	1.2835
1	2.1091	1.9328	1.8662	1.1615	1.2648	1.3078

Table 16. Skin Friction for isothermal plate for different values of *Pr* and *S*

***Pr*↓*Sc*→**	τ_{3x}			$-\tau_{3z}$		
	0.22	**0.6**	**0.78**	**0.22**	**0.6**	**0.78**
0.025	2.4229	2.2466	2.1799	1.0001	1.1034	1.1463
0.71	2.2051	2.0288	1.9621	1.1194	1.2228	1.2657
1	2.1427	1.9664	1.8997	1.1561	1.2595	1.3024

Table 17. Skin Friction for ramped temperature plate for different values of *N* and

N↓*t*→	τ_{3x}			$-\tau_{3z}$		
	0.5	**1.5**	**2.5**	**0.5**	**1.5**	**2.5**
1	2.5190	1.9729	1.6929	1.2371	1.2405	1.3921
3	2.5971	1.8915	1.6179	1.1908	1.2892	1.4373
5	2.6219	1.8653	1.5940	1.1750	1.3058	1.4525

Table 18. Skin Friction for isothermal plate for different values of *N* and *t t*

***N*↓*t*→**	τ_{3x}			$-\tau_{3z}$		
	0.5	**1.5**	**2.5**	**0.5**	**1.5**	**2.5**
1	2.4269	2.0288	1.7121	1.2700	1.2228	1.3850
3	2.4630	1.9662	1.6433	1.2426	1.2604	1.4264
5	2.4788	1.9462	1.6213	1.2350	1.2730	1.4402

Table 19. Effects of different flow parameters on Nusselt Number for both ramped temperature and isothermal plates and Sherwood Number

t	**Pr**	**Q**	**N**	**Sc**	**Kr**	**Nu**	**Nu_i**	**Sh**
0.5	0.71	1	1	0.6	1	0.9076	1.3335	0.9037
1.5	0.71	1	1	0.6	1	1.2985	1.2883	0.7897
2.5	0.71	1	1	0.6	1	1.2875	1.2872	0.7777
1.5	**0.1**	1	1	-	-	0.4873	0.4835	-
1.5	**0.3**	1	1	-	-	0.8440	0.8375	-
1.5	**0.71**	1	1	-	-	0.9076	1.2883	-
1.5	0.71	**1**	1	-	-	1.2985	1.2883	-
1.5	0.71	**3**	1	-	-	0.7497	0.7438	-
1.5	0.71	**5**	1	-	-	0.5807	0.5762	-
1.5	0.71	1	**1**	-	-	1.2985	1.2883	-
1.5	0.71	1	**3**	-	-	1.0429	1.0193	-
1.5	0.71	1	**5**	-	-	0.9858	0.9578	-
1.5	-	-	-	**0.22**	1	-	-	0.4782
1.5	-	-	-	**0.6**	1	-	-	0.7897
1.5	-	-	-	**0.8**	1	-	-	0.9004
1.5	-	-	-	0.6	**1**	-	-	0.7897
1.5	-	-	-	0.6	**3**	-	-	1.3420
1.5	-	-	-	0.6	**5**	-	-	1.7321

Table 20. Comparison of skin friction for $f(t)=H(t)$ with Nandkeolyar et al. [20]

T	**Q**	**Pr**	**M**	**Gr**	**Gm**	**Nandkeolyar et al. [20]**		**Present study**	
						τ_1	τ_{1i}	τ_1	τ_{1i}
0.3	1	0.71	3	2	2	-0.807404	-0.064685	-0.807404	-0.064685
0.5	1	0.71	3	2	2	-0.497522	0.1770467	-0.497422	0.1770477
0.7	1	0.71	3	2	2	-0.287319	0.2532688	-0.287419	0.2542688

Table 21. Comparison of skin friction for $f(t)=tH(t)$ with Nandkeolyar et al. [20]

T	Q	Pr	M	Gr	Gm	Nandkeolyar et al. [20]		Present Study	
						τ_2	τ_{2i}	τ_2	τ_{2i}
0.3	1	0.71	3	2	2	0.243499	0.986218	0.243499	0.986218
0.5	1	0.71	3	2	2	0.120771	0.795340	0.120671	0.795440
0.7	1	0.71	3	2	2	-0.04094	0.499646	-0.04194	0.499546

Table 22. Comparison of skin friction for $f(t)=\cos\omega tH(t)$ with Nandkeolyar et al. [20]

T	Q	Pr	M	Gr	Gm	Nandkeolyar et al. [20]		Present Study	
						τ_3	τ_{3i}	τ_3	τ_{3i}
0.3	1	0.71	3	2	2	-0.51381	0.228899	-0.51381	0.228899
0.5	1	0.71	3	2	2	0.234635	0.909204	0.234535	0.909104
0.7	1	0.71	3	2	2	0.980104	1.520692	0.980114	1.520792

6 Conclusion

An investigation of the effects of Hall current, rotation, chemical reaction and thermal radiation on unsteady MHD free convection heat and mass transfer flow of a viscous, incompressible, electrically conducting and heat absorbing fluids past an infinite flat plate embedded in a porous medium is carried out. The flow was induced by a time-dependent movement of the flat plate. Three cases of particular interest, namely (I) movement of the plate with uniform velocity (II) movement of the plate with uniform acceleration and (III) movement of the plate with periodic acceleration, have been discussed. Exact solutions of the governing equations were obtained using Laplace Transforms technique. A comprehensive set of graphical for the fluid velocity, fluid temperature and species concentration is presented and their dependence on some physical parameters for both ramped temperature and isothermal plates are discussed. Significant findings are as follows:

For both ramped temperature and isothermal plates

- Hall current and rotation tends to accelerate secondary fluid velocity throughout the boundary layer region whereas it has a reverse effect on the primary fluid velocity throughout the boundary layer region.
- Chemical reaction decelerates the fluid motion for both ramped temperature and isothermal plate which results in decreasing the fluid velocity throughout the boundary layer.
- Thermal boundary layer thickness decreases with an increase in the radiation parameter results in decrease in the primary and secondary fluid velocities for ramped temperature whereas it has reverse effect for isothermal plate.
- Time accelerate the fluid temperature whereas radiation parameter decreases the fluid temperature for ramped temperature and increases for isothermal plate.
- Mass diffusion and chemical reaction parameter tend to decrease the species concentration, whereas time has the reverse effect.
- Hall current and mass diffusion tend to decrease the primary skin friction for both ramped temperature and isothermal plate whereas it has reverse effect on secondary skin friction.
- Rotation tends to increase primary and secondary skin friction for both ramped temperature and isothermal plate.
- Thermal diffusion and time tends to enhance rate of heat transfer whereas it has reverse effect on secondary skin friction.
- Mass diffusion and chemical reaction tends to enhance the rate of mass transfer whereas as time progress the rate of mass transfer getting reduced.

Acknowledgements

The author's sincerely thank the reviewers for their valuable comments and suggestions which helped to improve the quality of the paper.

Competing Interests

The authors declare that they have no competing interests.

References

[1] Bejan A. Convection heat transfer. 2nd Ed. New York : Wiley; 1993.

[2] Gebhart B, Pera L. The nature of vertical natural convection flows resulting from the combined buoyancy effects of thermal and mass diffusion. Int. J. Heat Mass Transfer. 1971;14(12):2025–2050.

[3] Raptis AA. Free convection and mass transfer effects on the oscillatory flow past an infinite moving vertical isothermal plate with constant suction and heat sources. Astrophy. Space Sci. 1982;86(1):43–53.

[4] Bejan A, Khair KR. Heat and mass transfer by natural convection in a porous medium. Int. J. Heat Mass Transfer. 1985;28(5):909–918.

[5] Jang JY, Chang WJ. Buoyancy-induced inclined boundary layer flow in a porous medium resulting from combined heat and mass buoyancy effects. Int. Communication Heat Mass Transfer. 1988;15(1):17–30.

[6] Oreper GM, Szekely J. The effect of an externally imposed magnetic field on buoyancy driven flow in a rectangular cavity. J. Cryst. Growth. 1983;64(3):505–515.

[7] Hossain MA, Mandal AC. Mass transfer effects on the unsteady hydromagnetic free convection flow past an accelerated vertical porous plate. J. Phys D Appl. Phys. 1985;18(7):163–169.

[8] Jha BK. MHD free convection and mass transform flow through a porous medium. Astrophy Space Sci. 1991;175(2):283–289.

[9] Chen CH. Combined heat and mass transfer in MHD free convection from a vertical surface with ohmic heating and viscous dissipation. Int. J. Eng. Sci. 2004;42(7):699–713.

[10] Chamkha AJ. Unsteady MHD convective heat and mass transfer past a semi-infinite vertical permeable moving plate with heat absorption. Int. J. Eng. Sci. 2004;42(2):217–230.

[11] Eldabe NTM, Elbashbeshy EMA, Hasanin WSA, Elsaid EM. Unsteady motion of MHD viscous incompressible fluid with heat and mass transfer through porous medium near a moving vertical plate. Int. J. Energy Tech. 2011;35(3):1–11.

[12] Singh AK. MHD free-convection flow in the Stokes problem for a vertical porous plate in a rotating system. Astrophy Space Sci. 1983;95(2):283–289.

[13] Singh AK. MHD free convection flow past an accelerated vertical porous plate in a rotating fluid. Astrophy Space Sci. 1984;103(1):155–163.

[14] Raptis AA, Singh AK. Rotation effects on MHD free-convection flow past an accelerated vertical plate. Mech. Res. Communication. 1985;12(1):31–40.

[15] Singh AK, Singh NP, Singh U, Singh H. Convective flow past an accelerated porous plate in rotating system in presence of magnetic field. Int. J. Heat Mass Transfer. 2009;52(13-14):3390–3395.

[16] Muthucumaraswamy R, Valli-Ammal V. The theoretical study of unsteady flow past an exponentially accelerated infinite isothermal vertical plate with variable mass diffusion in the presence of homogeneous chemical reaction of first order. Theo. Appl. Mech. 2010;37(4):251– 262.

[17] Sarma D, Pandit KK. Effects of thermal radiation and chemical reaction on steady MHD mixed convective flow over a vertical porous plate with induced magnetic field. Int. J. of Fluid Mech. Res. 2015;42(4):315-333.

[18] Suneetha S, Bhaskar Reddy N, Ramachandra Prasad V. Effects of thermal radiation on the natural convective heat and mass transfer of a viscous incompressible gray absorbing-emitting fluid flowing past an impulsively started moving vertical plate with viscous dissipation. Thermal Science. 2009;13(2):71–181.

[19] Satter MA, Kalim H. Unsteady free-convection interaction with thermal radiation in a boundary layer flow past a vertical porous plate. J. Math. Phys. Sci. 1996;30(1):25- 37.

[20] Nandkeolyar R, Das M, Sibanda P. Exact solutions of unsteady MHD free convection in a heat absorbing fluid flow past a flat plate with ramped wall temperature. Boundary Value Problems. 2013;1:1-16.

[21] Cramer KR, Pai SI. Magneto fluid dynamics for engineers and applied physicists, New York: McGraw Hill Book Company; 1973.

[22] Pop I, Watanabe T. Hall Effect on magneto hydrodynamic free convection about a semi-infinite vertical flat plate. Int. J. Eng. Sci. 1994;32(12):1903–1911.

[23] Takhar HS, Roy S, Nath G. Unsteady free convection flow over an infinite vertical porous plate due to the combined effects of thermal and mass diffusion, magnetic field and Hall currents. Heat Mass Transfer. 2003;39(10):825–834.

[24] Saha LK, Siddiqa S, Hossain MA. Effect of Hall current on MHD natural convection flow from vertical permeable flat plate with uniform surface heat flux. Appl. Math Mech. Eng. Ed. 2011;32(9):1127–1146.

[25] Satya Narayana PV, Venkateswarlu B, Venkataramana S. Effects of Hall current and radiation absorption on MHD micropolar fluid in a rotating system. Ain Shams Eng. J. 2013;4(4):843–854.

[26] Sarma D, Pandit KK. Effects of Hall current, rotation and Soret effects on MHD free convection heat and mass transfer flow past an accelerated vertical plate through a porous medium. Ain Shams Eng. J; 2016 (in Press).
DOI: 10.1016/j.asej.2016. 03.005

[27] Seth GS, Mahato GK, Sarkar S. Effects of Hall current and rotation on MHD natural convection flow past an impulsively moving vertical plate with ramped temperature in the presence of thermal diffusion with heat absorption. Int. J. Energy Tech. 2013;5(16):1–12.

[28] Seth GS, Sarkar S, Hussain SM. Effects of Hall current, radiation and rotation on natural convection heat and mass transfer flow past a moving vertical plate. Ain Shams Eng. J. 2014;5(2):489–503.

[29] Takhar HS, Chamkha AJ, Nath G. MHD flow over a moving plate in a rotating fluid with magnetic field, Hall currents and free stream velocity. Int. J. of Eng. Sci. 2002;40(13):1511-1527.

[30] Jaber KK. Effect of Hall currents and variable fluid properties on MHD flow past stretching vertical plate by the presence of radiation. J. of Appl. Mathematics and Physics. 2014;2:888-902.

[31] Ghara N, Maji SL, Das S, Jana R, Ghosh SK. Effects of Hall Current and Ion-Slip on unsteady MHD Couette flow. Open J. of Fluid Dynamics. 2012;2:1-13.

[32] Guchhait SK, Das S, Jana RN. Combined effects of Hall current and radiation on MHD free convective flow in a vertical channel with an oscillatory wall temperature. Open J. of Fluid Dynamics. 2013;3:9-22.

[33] Satya Narayana PV, Venkateswarlu B, Venkataramana S. Effects of Hall current and radiation absorption on MHD micropolar fluid in a rotating system. Ain Shams Engineering J. 2013;4:843-854.

[34] Anika NN, Hoque MM, Islam N. Hall current effects on magneto hydrodynamics fluid over an infinite Rotating vertical porous plate embedded in unsteady laminar flow. Annals of Pure and Appl. Mathematics. 2013;3(2):189-200.

[35] Anika NN, Hoque MM. Thermal buoyancy force effects on developed flow considering Hall and Ion-slip current. Annals of Pure and Appl. Mathematics. 08/2013;3(2):179-188.

[36] Seth GS, Sarkar S, Sharma R. Effects of Hall current on unsteady hydromagnetic free convection flow past an impulsively moving vertical plate with Newtonian heating. Int. J. of Appl. Mech. and Eng. 2016;21(1): 187-203.

[37] Cowling TG. Magneto hydrodynamics. New York: Inderscience Publishers; 1957.

[38] Meyer RC. On reducing aerodynamic heat-transfer rates by magneto hydrodynamic techniques. J. Aeronaut. Sci. 1958;25:561-572.

[39] Sparrow EM and Cess RD. Radiation Heat Transfer. Washington DC: Hemisphere Publishing Corporation; 1978.

Appendix

$$\alpha_1=\frac{\lambda Gr}{A_1},\alpha_2=\frac{Gm}{A_3},A_1=\Pr-\lambda,A_2=\lambda\alpha-\Pr Q,A_3=Sc-1,A_4=\alpha-ScKr,\ A_5=\frac{A_2}{A_1},A_6=\frac{A_4}{A_3}.$$

$$P_1(y,t)=\frac{e^{A_5t}}{2A_5^2}\left\{\begin{array}{l}e^{y\sqrt{\alpha+A_5}}erfc\left(\frac{y}{2\sqrt{t}}+\sqrt{(\alpha+A_5)t}\right)+e^{-y\sqrt{\alpha+A_5}}erfc\left(\frac{y}{2\sqrt{t}}-\sqrt{(\alpha+A_5)t}\right)-\\ e^{y\sqrt{\frac{\Pr}{\lambda}(A_5+Q)}}erfc\left(\frac{y}{2}\sqrt{\frac{\Pr}{\lambda t}}+\sqrt{(A_5+Q)t}\right)-e^{-y\sqrt{\frac{\Pr}{\lambda}(A_5+Q)}}erfc\left(\frac{y}{2}\sqrt{\frac{\Pr}{\lambda t}}-\sqrt{(A_5+Q)t}\right)\end{array}\right\}$$

$$-\frac{1}{2A_5}\left(\frac{1}{A_5}+t+\frac{y}{2\sqrt{\alpha}}\right)e^{y\sqrt{\alpha}}erfc\left(\frac{y}{2\sqrt{t}}+\sqrt{\alpha t}\right)-\frac{1}{2A_5}\left(\frac{1}{A_5}+t-\frac{y}{2\sqrt{\alpha}}\right)e^{-y\sqrt{\alpha}}erfc\left(\frac{y}{2\sqrt{t}}-\sqrt{\alpha t}\right)+$$

$$\frac{1}{2A_5}\left(\frac{1}{A_5}+t+\frac{y}{2}\sqrt{\frac{\Pr}{\lambda Q}}\right)e^{y\sqrt{\frac{\Pr Q}{\lambda}}}erfc\left(\frac{y}{2}\sqrt{\frac{\Pr}{\lambda t}}+\sqrt{Qt}\right)+\frac{1}{2A_5}\left(\frac{1}{A_5}+t-\frac{y}{2}\sqrt{\frac{\Pr}{\lambda Q}}\right)e^{-y\sqrt{\frac{\Pr Q}{\lambda}}}erfc\left(\frac{y}{2}\sqrt{\frac{\Pr}{\lambda t}}-\sqrt{Qt}\right)$$

$$P_2(y,t)=\frac{e^{A_6t}}{2A_6}\left\{\begin{array}{l}e^{y\sqrt{\alpha+A_6}}erfc\left(\frac{y}{2\sqrt{t}}+\sqrt{(\alpha+A_6)t}\right)+e^{-y\sqrt{\alpha+A_6}}erfc\left(\frac{y}{2\sqrt{t}}-\sqrt{(\alpha+A_6)t}\right)-\\ e^{y\sqrt{(A_6+Kr)Sc}}erfc\left(\frac{y}{2}\sqrt{\frac{Sc}{t}}+\sqrt{(A_6+Kr)t}\right)-e^{-y\sqrt{(A_6+Kr)Sc}}erfc\left(\frac{y}{2}\sqrt{\frac{Sc}{t}}-\sqrt{(A_6+Kr)t}\right)\end{array}\right\}$$

$$-\frac{1}{2A_6}\left\{e^{y\sqrt{\alpha}}erfc\left(\frac{y}{2\sqrt{t}}+\sqrt{\alpha t}\right)+e^{-y\sqrt{\alpha}}erfc\left(\frac{y}{2\sqrt{t}}-\sqrt{\alpha t}\right)\right\}+$$

$$\frac{1}{2A_6}\left\{e^{y\sqrt{KrSc}}erfc\left(\frac{y}{2}\sqrt{\frac{Sc}{t}}+\sqrt{Krt}\right)+e^{-y\sqrt{KrSc}}erfc\left(\frac{y}{2}\sqrt{\frac{Sc}{t}}-\sqrt{Krt}\right)\right\}$$

$$P_3(y,t)=\frac{e^{A_5t}}{2A_5}\left\{\begin{array}{l}e^{y\sqrt{\alpha+A_5}}erfc\left(\frac{y}{2\sqrt{t}}+\sqrt{(\alpha+A_5)t}\right)+e^{-y\sqrt{\alpha+A_5}}erfc\left(\frac{y}{2\sqrt{t}}-\sqrt{(\alpha+A_5)t}\right)-\\ e^{y\sqrt{\frac{\Pr}{\lambda}(A_5+Q)}}erfc\left(\frac{y}{2}\sqrt{\frac{\Pr}{\lambda t}}+\sqrt{(A_5+Q)t}\right)-e^{-y\sqrt{\frac{\Pr}{\lambda}(A_5+Q)}}erfc\left(\frac{y}{2}\sqrt{\frac{\Pr}{\lambda t}}-\sqrt{(A_5+Q)t}\right)\end{array}\right\}$$

$$-\frac{1}{2A_5}\left\{\begin{array}{l}e^{y\sqrt{\alpha}}erfc\left(\frac{y}{2\sqrt{t}}+\sqrt{\alpha t}\right)+e^{-y\sqrt{\alpha}}erfc\left(\frac{y}{2\sqrt{t}}-\sqrt{\alpha t}\right)-\\ e^{y\sqrt{\frac{\Pr Q}{\lambda}}}erfc\left(\frac{y}{2}\sqrt{\frac{\Pr}{\lambda t}}+\sqrt{Qt}\right)-e^{-y\sqrt{\frac{\Pr Q}{\lambda}}}erfc\left(\frac{y}{2}\sqrt{\frac{\Pr}{\lambda t}}-\sqrt{Qt}\right)\end{array}\right\}$$

$$P_4(y,t)=\frac{1}{2}\left[e^{y\sqrt{\alpha}}erfc\left(\frac{y}{2\sqrt{t}}+\sqrt{\alpha t}\right)+e^{-y\sqrt{\alpha}}erfc\left(\frac{y}{2\sqrt{t}}-\sqrt{\alpha t}\right)\right]$$

$$P_5(y,t)=\left(\frac{t}{2}+\frac{y}{4\sqrt{\alpha}}\right)e^{y\sqrt{\alpha}}erfc\left(\frac{y}{2\sqrt{t}}+\sqrt{\alpha t}\right)+\left(\frac{t}{2}-\frac{y}{4\sqrt{\alpha}}\right)e^{-y\sqrt{\alpha}}erfc\left(\frac{y}{2\sqrt{t}}-\sqrt{\alpha t}\right)$$

$$P_6(y,t)=\frac{1}{4}e^{-i\omega t}\left\{e^{y\sqrt{\alpha-i\omega}}erfc\left(\frac{y}{2\sqrt{t}}+\sqrt{(\alpha-i\omega)t}\right)+e^{-y\sqrt{\alpha-i\omega}}erfc\left(\frac{y}{2\sqrt{t}}-\sqrt{(\alpha-i\omega)t}\right)\right\}+$$

$$\frac{1}{4}e^{i\omega t}\left\{e^{y\sqrt{\alpha+i\omega}}erfc\left(\frac{y}{2\sqrt{t}}+\sqrt{(\alpha+i\omega)t}\right)+e^{-y\sqrt{\alpha+i\omega}}erfc\left(\frac{y}{2\sqrt{t}}-\sqrt{(\alpha+i\omega)t}\right)\right\}$$

$$\theta_1(y,t)=\frac{1}{2}\left[\left(t+\frac{y}{2}\sqrt{\frac{\Pr}{\lambda Q}}\right)e^{y\sqrt{\frac{\Pr Q}{\lambda}}}erfc\left(\frac{y}{2}\sqrt{\frac{\Pr}{\lambda t}}+\sqrt{Qt}\right)+\left(t-\frac{y}{2}\sqrt{\frac{\Pr}{\lambda Q}}\right)e^{-y\sqrt{\frac{\Pr Q}{\lambda}}}erfc\left(\frac{y}{2}\sqrt{\frac{\Pr}{\lambda t}}-\sqrt{Qt}\right)\right]$$

$$\theta_2(0,t)=-\left[t\sqrt{\frac{\Pr Q}{\lambda}}erf\left(\sqrt{Qt}\right)+\frac{1}{2}\sqrt{\frac{\Pr}{\lambda Q}}erf\left(\sqrt{Qt}\right)+t\sqrt{\frac{\Pr}{\pi\lambda t}}e^{-Qt}\right]$$

$$Q_1(t)=-\sqrt{\alpha}erf\left(\sqrt{\alpha t}\right)-\frac{1}{\sqrt{\pi t}}e^{-\alpha t},\ Q_2(t)=-\left(\frac{1}{2\sqrt{\alpha}}+t\sqrt{\alpha}\right)erf\left(\sqrt{\alpha t}\right)-\sqrt{\frac{t}{\pi}}e^{-\alpha t}$$

$$Q_3(t)=-\frac{e^{-\alpha t}}{\sqrt{\pi t}}-\frac{1}{2}\sqrt{\alpha-i\omega}e^{-i\omega t}erf\left(\sqrt{(\alpha-i\omega)t}\right)-\frac{1}{2}\sqrt{\alpha+i\omega}e^{i\omega t}erf\left(\sqrt{(\alpha+i\omega)t}\right)$$

$$F_1(t)=\frac{e^{A_5 t}}{A_5^2}\left\{\begin{array}{l}-\sqrt{(\alpha+A_5)}erf\left(\sqrt{(\alpha+A_5)t}\right)-\frac{1}{\sqrt{\pi t}}e^{-(\alpha+A_5)t}+\\ \sqrt{\frac{\Pr}{\lambda}(A_5+Q)}erf\left(\sqrt{(A_5+Q)t}\right)+\sqrt{\frac{\Pr}{\pi\lambda t}}e^{-(A_5+Q)t}\end{array}\right\}-$$

$$\frac{1}{A_5}\left\{\begin{array}{l}-\frac{1}{2\sqrt{\alpha}}erf\left(\sqrt{\alpha t}\right)-\sqrt{\alpha}\left(\frac{1}{A_5}+t\right)erf\left(\sqrt{\alpha t}\right)-\frac{1}{\sqrt{\pi t}}\left(\frac{1}{A_5}+t\right)e^{-\alpha t}+\\ \frac{1}{2}\sqrt{\frac{\Pr}{\lambda Q}}erf\left(\sqrt{Qt}\right)+\left(\frac{1}{A_5}+t\right)\sqrt{\frac{\Pr Q}{\lambda}}erf\left(\sqrt{Qt}\right)+\left(\frac{1}{A_5}+t\right)\sqrt{\frac{\Pr}{\pi\lambda t}}e^{-Qt}\end{array}\right\}$$

$$F_2(t)=\frac{e^{A_6 t}}{A_6}\left\{\begin{array}{l}-\sqrt{(\alpha+A_6)}erf\left(\sqrt{(\alpha+A_6)t}\right)-\frac{1}{\sqrt{\pi t}}e^{-(\alpha+A_6)t}+\\ \sqrt{(A_6+Kr)Sc}erf\left(\sqrt{(A_6+Kr)t}\right)+\sqrt{\frac{Sc}{\pi t}}e^{-(A_6+Kr)t}\end{array}\right\}+\frac{1}{A_6}\left\{\begin{array}{l}\sqrt{\alpha}erf\left(\sqrt{\alpha t}\right)+\frac{1}{\sqrt{\pi t}}e^{-\alpha t}-\\ \sqrt{KrSc}erf\left(\sqrt{Krt}\right)-\sqrt{\frac{Sc}{\pi t}}e^{-Krt}\end{array}\right\}$$

$$F_3(t)=\frac{e^{A_5 t}}{A_5}\left\{\begin{array}{l}-\sqrt{(\alpha+A_5)}erf\left(\sqrt{(\alpha+A_5)t}\right)-\frac{1}{\sqrt{\pi t}}e^{-(\alpha+A_5)t}+\\ \sqrt{\frac{\Pr}{\lambda}(A_5+Q)}erf\left(\sqrt{(A_5+Q)t}\right)+\sqrt{\frac{\Pr}{\pi\lambda t}}e^{-(A_5+Q)t}\end{array}\right\}+\frac{1}{A_5}\left\{\begin{array}{l}\sqrt{\alpha}erf\left(\sqrt{\alpha t}\right)+\frac{1}{\sqrt{\pi t}}e^{-\alpha t}-\\ \sqrt{\frac{\Pr Q}{\lambda}}erf\left(\sqrt{Qt}\right)-\sqrt{\frac{\Pr}{\pi\lambda t}}e^{-Qt}\end{array}\right\}$$

Peer-review history:
The peer review history for this paper can be accessed here (Please copy paste the total link in your browser address bar)
http://sciencedomain.org/review-history/16081